Electronic Supplementary Material (ESI) for Journal of Materials Chemistry A.

Supporting Information

Title: Nickel Sulfide Nanospheres Anchored on Reduced Graphene Oxide *in-situ* Doped with Sulfur as High Performance Anode for Sodium-ion Batteries

Hongwei Tao, Min Zhou*, Kangli Wang*, Shijie Cheng and Kai Jiang*

1. Elemental composition information of the NiS_x-rGOS-1, NiS_x-rGOS-2 and NiS_x-rGOS-3

Table S1 Elemental composition information of the NiS_x-rGOS-1, NiS_x-rGOS-2 and NiS_x-rGOS-3

Sample	C(wt%)	S(wt%)	H(wt%)
NiS_x-rGOS-1	26.7	25.2	0.9
NiS_x-rGOS-2	43.9	22.0	1.6
NiS_x-rGOS-3	64.9	12.0	2.2

2. XRD patterns of NiS_x, NiS_x-rGOS-1, NiS_x-rGOS-2 and NiS_x-rGOS-3 before calcination

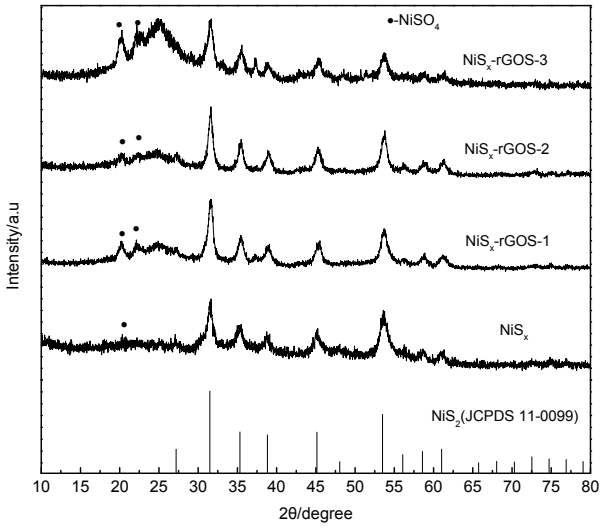

Fig. S1 XRD patterns of NiS_x, NiS_x-rGOS-1, NiS_x-rGOS-2 and NiS_x-rGOS-3 before calcination

3. FT-IR and Raman spectras of rGO.

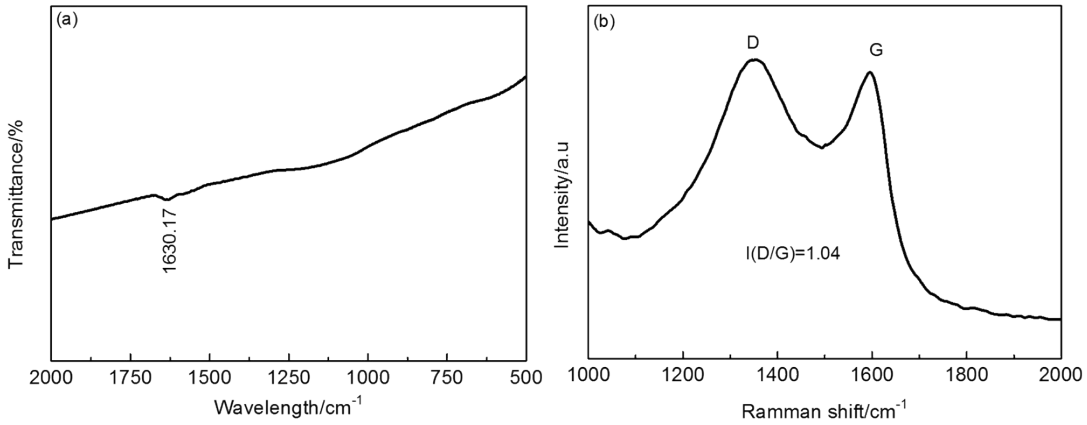

Fig. S2 FT-IR (a) and Raman (b) spectras of rGO.

4. Raman spectras of GO, NiS_x, NiS_x-rGOS-1, NiS_x-rGOS-2 and NiS_x-rGOS-3

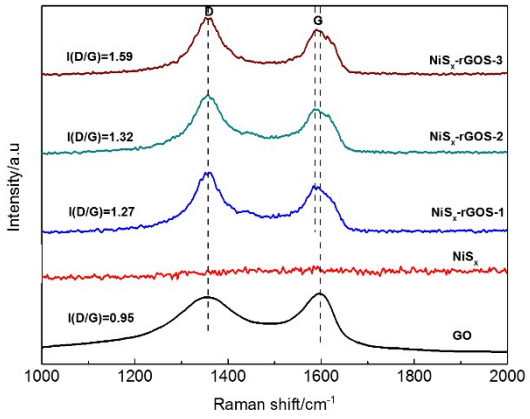

Fig. S3 Raman spectras of GO, NiS_x, NiS_x-rGOS-1, NiS_x-rGOS-2 and NiS_x-rGOS-3

5. **X-ray photoelectron spectroscopic (XPS) spectra of NiS_x-rGOS.**

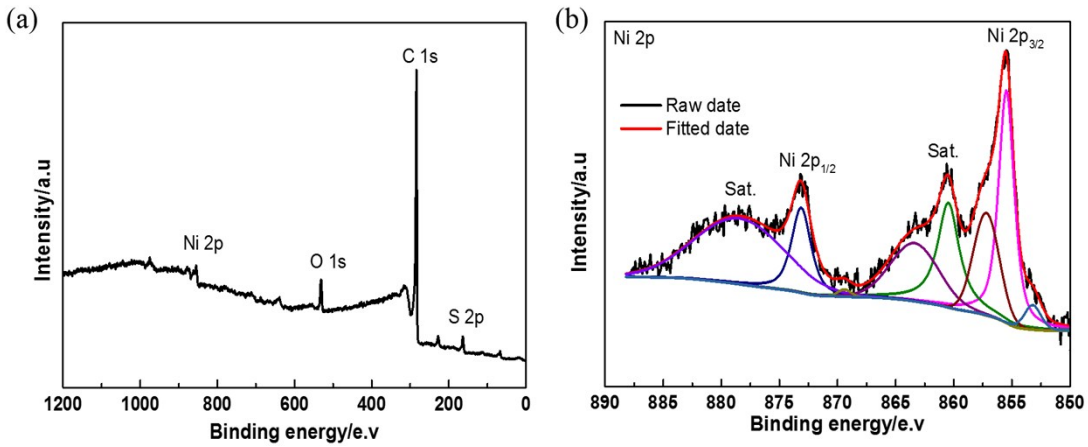

Fig. S4 Typical XPS spectra of the NiS_x-rGOS-1 composite: (a) survey spectra, (b) Ni 2p region XPS spectrum

6. N_2 adsorption–desorption isotherm of the as prepared NiS_x, NiS_x-rGOS-1, NiS_x-rGOS-2 and NiS_x-rGOS-3

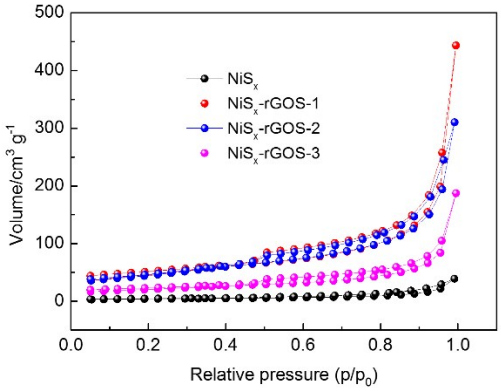

Fig. S5 N_2 adsorption–desorption isotherm of the as prepared NiS_x, NiS_x-rGOS-1, NiS_x-rGOS-2 and NiS_x-rGOS-3

7. **SEM images of NiS_x, NiS_x-rGOS-1, NiS_x-rGOS-2 and NiS_x-rGOS-3 before calcination.**

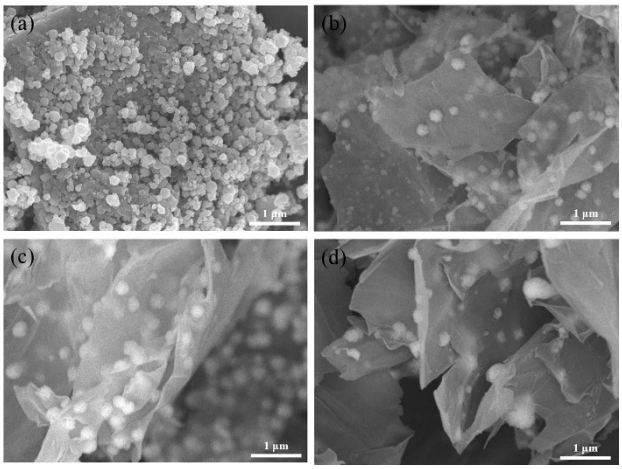

Fig. S6 SEM images of NiS_x (a), NiS_x-rGOS-1(b), NiS_x-rGOS-2 (c) and NiS_x-rGOS-3 (d) before calcination.

8. TEM and HRTEM images of NiS_x-rGOS-2 and NiS_x-rGOS-3

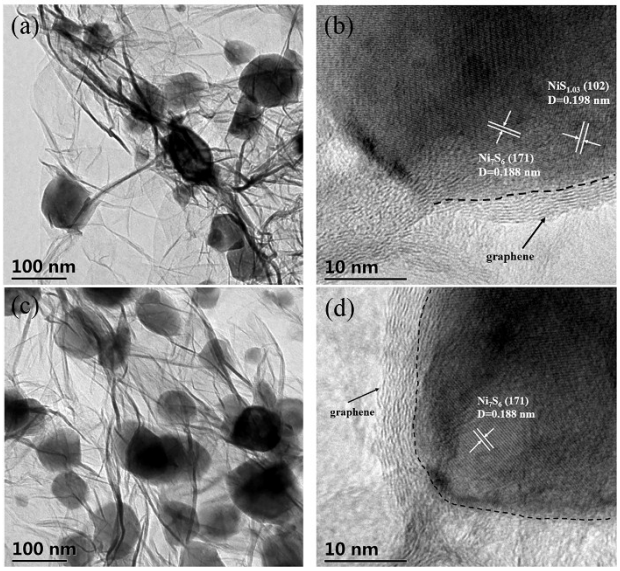

Fig. S7 TEM and HRTEM images of NiS_x-rGOS-2 (a-b) and NiS_x-rGOS-3 (c-d).

9. CV curves of rGOS.

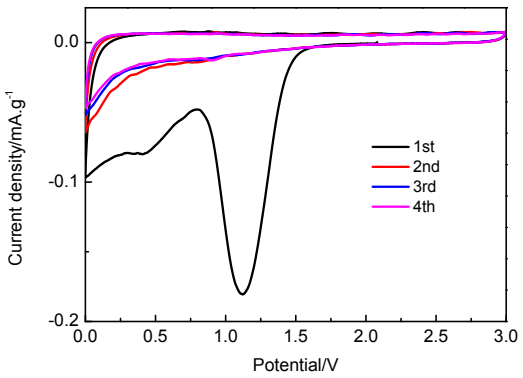

Fig. S8 CV curves of rGOS.

In Fig.S8, during the first cathodic sweep, the irreversible peak at 1.1V is attributed to the side reactions of the function groups on the surface of the rGO, and the cathodic peak at 0.6 V is assigned to the decomposition of the electrolyte to form a solid-electrolyte interface (SEI). In the subsequent scans, a pair of redox peaks at ~ 0.1 V can be ascribed to the reversible insertion/extraction of Na^+ into/from the rGO. Based on the CV curves of the rGO, the redox peaks near 0.1 V for the NiS_x-rGOS-3 can be ascribed to the insertion/extraction of Na^+ of the rGOS.

10. Electrochemical performances of rGO and rGOS

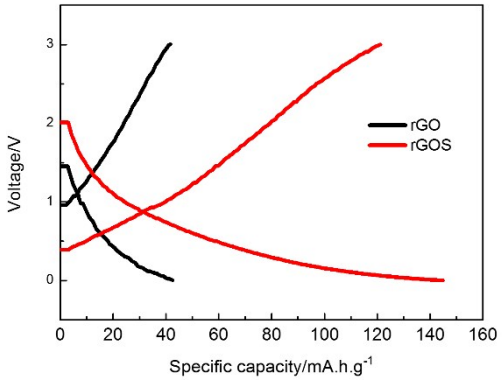

Fig. S9 Charge-discharge profiles for the rGO and rGOS at the current density of 0.2 A g^{-1}.

As shown in Fig.S9, the rGOS electrode exhibit a high reversible capacity of 134 mAh g^{-1} at the current densities of 0.2 A g^{-1} due to the sulfur doped into rGO. For comparison, the rGO electrode only delivery a capacity of 43 mAh g^{-1}.

11. S 2p XPS spectra of the cycled NiS_x-rGOS-1 electrode.

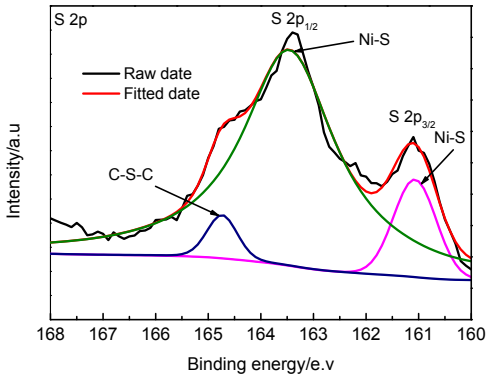

Fig. S10 S 2p XPS spectra of the cycled NiS_x-rGOS-1 electrode.

12. Raw and fitting electrochemical impedance spectra (EIS) of the NiS_x and NiS_x-rGOS electrode after cycling

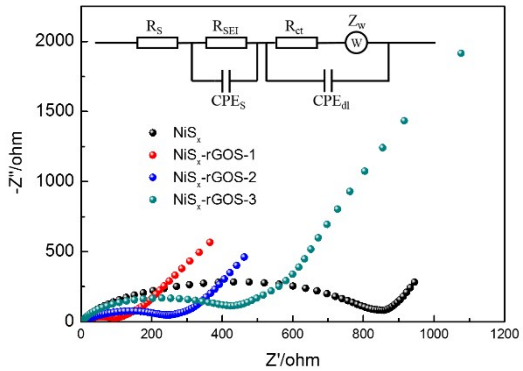

Fig.S11 Nyquist plots of NiS_x, NiS_x-rGOS-1, NiS_x-rGOS-2 and NiS_x-rGOS-3. Inset is the corresponding equivalent circuit model.

Table S2 Fitting results of the Nyquist plots using the equivalent circuit.

samples	R_S (Ω)	R_{SEI} (Ω)	CPE_S(F)	R_{ct}(Ω)	CPE_{dl}(F)	Chi-Squared
NiS_x	2.6	99.3	7.4×10^{-6}	704.8	7.4×10^{-5}	5.0×10^{-3}
NiS_x-rGOS-1	3.1	5.0	5.1×10^{-6}	84.1	3.7×10^{-5}	2.9×10^{-3}
NiS_x-rGOS-2	4.3	15.0	4.5×10^{-6}	176.3	2.5×10^{-5}	1.3×10^{-3}
NiS_x-rGOS-3	2.1	45.4	3.9×10^{-6}	225.4	5.3×10^{-6}	2.9×10^{-3}

13. SEM and TEM images of pristine and cycled electrodes NiS_x and NiS_x-rGOS-1

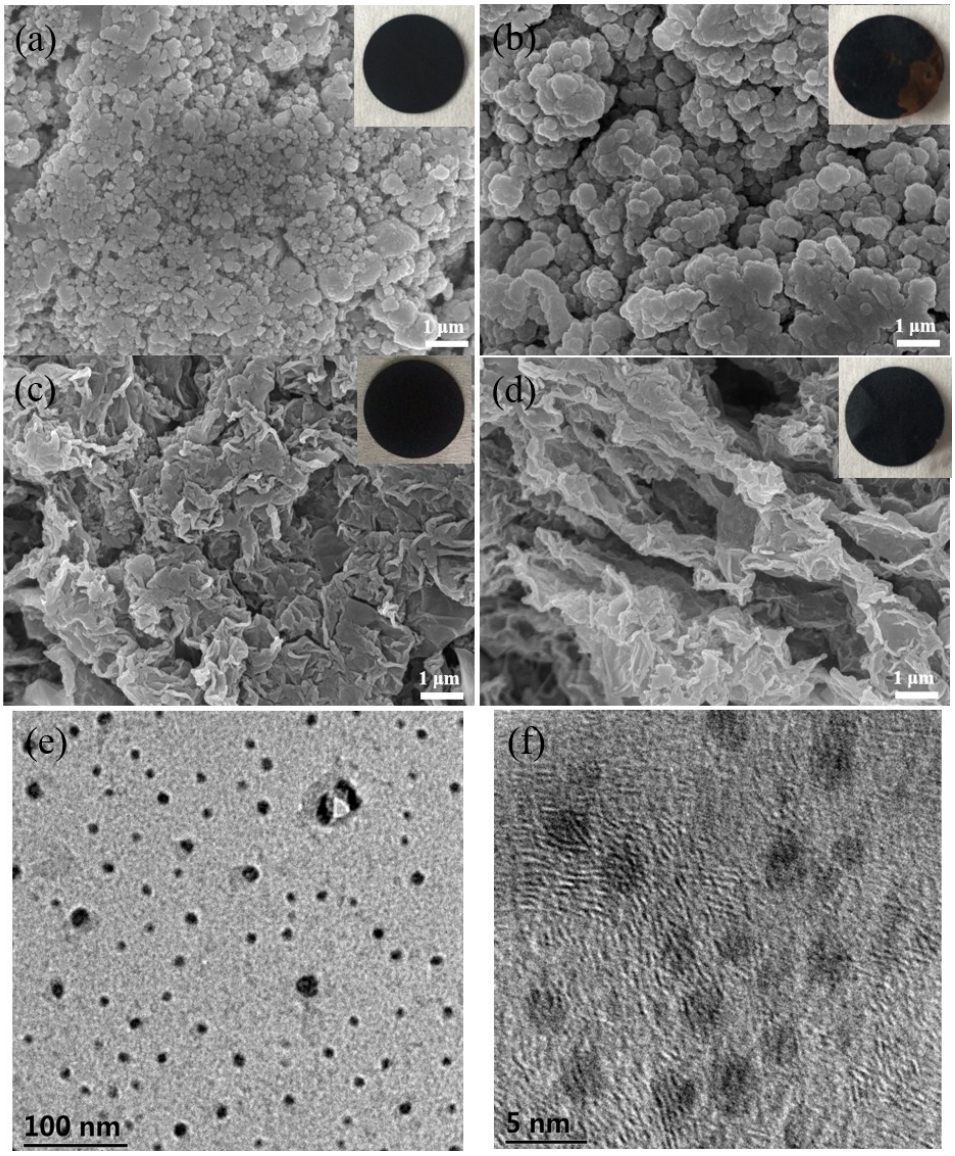

Fig. S12 SEM images of pristine and cycled electrodes (100 cycle) (a-b)NiS_x, and (c-d) NiS_x-rGOS-1, (e-f) HRTEM images of NiS_x-rGOS-1 electrodes after 100 cycles at 0.2 A g^{-1}. Insets: corresponding digital photographs.

14. Comparison of the results in this study with those of previously reported in the literature.

Table S3 comparison of the results in this study with those of previously reported in the literature.

Anode	Capacity/Current density	Cycle number/capacity retention	Reference
NiSx-rGOS	515 mA h g^{-1}/0.2 A g^{-1} 414 mA h g^{-1}/4 A g^{-1}	100/96.8%	This work
Nano hollow NiS_x-rGO	504 mA h g^{-1}/0.2 A g^{-1} 377 mA h g^{-1}/3 A g^{-1}	150/100%	[1]
hierarchical hollow α-NiS spheres	499.9 mA h g^{-1}/0.1 A g^{-1} 337.4 mA h g^{-1}/5 A g^{-1}	50/73%	[2]
Nickel sulphide-RGO composites	513 mA h g^{-1}/0.1 A g^{-1} 346 mA h g^{-1}/1 A g^{-1}	50/88.4%	[3]
NiS_x/CNT@C	406 mA h g^{-1}/0.2 A g^{-1} 143 mA h g^{-1}/5 A g^{-1}	200/85%	[4]
NiS_2-GNS	382 mA h g^{-1}/0.1C 168 mA h g^{-1}/2C(1C=807 mA g^{-1})	200/77%	[5]
Ni_3S_2/Ni	315.3 mA h g^{-1}/0.05 A g^{-1}	100/90.6%	[6]
Ni_3S_2-PEDOT	600 mA h g^{-1}/0.15 A g^{-1} 310 mA h g^{-1}/1.2 A g^{-1}	50/60%	[7]
CNT@NiS/C	600 mA h g^{-1}/0.1 A g^{-1}	100/98%	[8]
Ni_3S_2/graphene	284 mA h g^{-1}/0.6 A g^{-1}	110/71.1%	[9]

1. Park, G.D., J.S. Cho, and Y.C. Kang, *Sodium-ion storage properties of nickel sulfide hollow nanospheres/reduced graphene oxide composite powders prepared by a spray drying process and the nanoscale Kirkendall effect.* Nanoscale, 2015. **7**(40): p. 16781-8.
2. Zhang, D., et al., *Engineering Hierarchical Hollow Nickel Sulfide Spheres for High-Performance Sodium Storage.* Advanced Functional Materials, 2016.
3. Qin, W., et al., *Layered nickel sulfide-reduced graphene oxide composites synthesized via microwave-assisted method as high performance anode materials of sodium-ion batteries.* Journal of Power Sources, 2016. **302**: p. 202-209.
4. Zhao, F., et al., *Stabilizing nickel sulfide nanoparticles with an ultrathin carbon layer for improved cycling performance in sodium ion batteries.* Nano Research, 2016. **9**(10): p. 3162-3170.
5. Wang, T., et al., *Nickel Disulfide-Graphene Nanosheets Composites with Improved Electrochemical Performance for Sodium Ion Battery.* ACS Appl Mater Interfaces, 2016. **8**(12): p. 7811-7.
6. Song, X., et al., *Morphology-dependent performance of nanostructured Ni3S2/Ni anode electrodes for high performance sodium ion batteries.* Nano Energy, 2016. **26**: p. 533-540.
7. Shang, C., et al., *A Ni3S2-PEDOT monolithic electrode for sodium batteries.* Electrochemistry Communications, 2015. **50**: p. 24-27.
8. Han, F., C.Y.J. Tan, and Z. Gao, *A Dual-Carbon Phase-Modified and Nanostructured Nickel Sulfide Anode for Sodium-Ion Batteries.* Energy Technology, 2017.
9. Xia, X., et al., *Wrinkled Graphene-Reinforced Nickel Sulfide Thin Film as High-Performance Binder-Free Anode for Sodium-Ion Battery.* Journal of Materials Science & Technology, 2016.